Nanoscale plasmonic contour bowtie antenna operating in the mid-infrared

S. Sederberg* and A. Y. Elezzabi

Department of Electrical and Computer Engineering, University of Alberta, Edmonton, Alberta, T6G 2V4, Canada
**shawns@ualberta.ca*

Abstract: A plasmonic antenna design is proposed and investigated numerically over a large parameter space. By considering the contour of a bowtie antenna and introducing an additional design parameter, the contour thickness, it is demonstrated that the resonant wavelength of the antenna may be tuned over a broad spectral range while maintaining a constant antenna footprint. These new antennas allow for a factor of 3.6 reduction in the antenna footprint and an increase in the gap enhancement by 28%.

OCIS codes: (250.5403) Plasmonics; (350.4238) Nanophotonics and photonic crystals; (260.3910) Metal optics; (310.6628) Subwavelength structures, nanostructures; (140.4780) Optical resonators; (260.5740) Resonance.

References and links

1. L. Wang and X. Xu, "High transmission nanoscale bowtie-shaped aperture probe for near-field optical imaging," Appl. Phys. Lett. **90**(26), 261105 (2007).
2. S. Aksu, A. A. Yanik, R. Adato, A. Artar, M. Huang, and H. Altug, "High-throughput nanofabrication of infrared plasmonic nanoantenna arrays for vibrational nanospectroscopy," Nano Lett. **10**(7), 2511–2518 (2010).
3. F. Neubrech, A. Pucci, T. W. Cornelius, S. Karim, A. García-Etxarri, and J. Aizpurua, "Resonant plasmonic and vibrational coupling in a tailored nanoantenna for infrared detection," Phys. Rev. Lett. **101**(15), 157403 (2008).
4. R. Adato, A. A. Yanik, J. J. Amsden, D. L. Kaplan, F. G. Omenetto, M. K. Hong, S. Erramilli, and H. Altug, "Ultra-sensitive vibrational spectroscopy of protein monolayers with plasmonic nanoantenna arrays," Proc. Natl. Acad. Sci. U.S.A. **106**(46), 19227–19232 (2009).
5. S. Kim, J. Jin, Y. J. Kim, I. Y. Park, Y. Kim, and S. W. Kim, "High-harmonic generation by resonant plasmon field enhancement," Nature **453**(7196), 757–760 (2008).
6. N. Yu, E. Cubukcu, L. Diehl, D. Bour, S. Corzine, J. Zhu, G. Höfler, K. B. Crozier, and F. Capasso, "Bowtie plasmonic quantum cascade laser antenna," Opt. Express **15**(20), 13272–13281 (2007).
7. K. D. Ko, A. Kumar, K. H. Fung, R. Ambekar, G. L. Liu, N. X. Fang, and K. C. Toussaint, Jr., "Nonlinear optical response from arrays of Au bowtie nanoantennas," Nano Lett. **11**(1), 61–65 (2011).
8. A. Alù and N. Engheta, "Input impedance, nanocircuit loading, and radiation tuning of optical nanoantennas," Phys. Rev. Lett. **101**(4), 043901 (2008).
9. A. Alù and N. Engheta, "Tuning the scattering response of optical nanoantennas with nanocircuit loads," Nat. Photonics **2**(5), 307–310 (2008).
10. R. D. Averitt, D. Sarkar, and N. J. Halas, "Plasmon resonance shifts of Au-coated Au_2S nanoshells: insight into multicomponent nanoparticle growth," Phys. Rev. Lett. **78**(22), 4217–4220 (1997).
11. Y.-F. Chau, H.-H. Yeh, and D. P. Tsai, "A new type of optical antenna: plasmonics nanoshell bowtie antenna with dielectric hole," J. Electromagn. Waves Appl. **24**(11), 1621–1632 (2010).
12. Y.-F. Chau, H.-H. Yeh, and D. P. Tsai, "Surface plasmon resonances effects on different patterns of solid-silver and silver-shell nanocylindrical pairs," J. Electromagn. Waves Appl. **24**(8), 1005–1014 (2010).
13. Y.-F. Chau and H.-H. Yeh, "A comparative study of solid-silver and silver-shell nanodimers on surface plasmon resonances," J. Nanopart. Res. **13**(2), 637–644 (2011).
14. L. Wang, L. Cai, J. Zhang, W. Bai, H. Hu, and G. Song, "Design of plasmonic bowtie nanoring array with high sensitivity and reproducibility for surface-enhanced Raman scattering spectroscopy," J. Raman Spectrosc **42**(6), 1263–1266 (2011).
15. L. Novotny, "Effective wavelength scaling for optical antennas," Phys. Rev. Lett. **98**(26), 266802 (2007).
16. M. Schnell, A. Garcia-Etxarri, A. J. Huber, K. Crozier, J. Aizpurua, and R. Hillenbrand, "Controlling the near-field oscillations of loaded plasmonic nanoantennas," Nat. Photonics **3**(5), 287–291 (2009).
17. H. Fischer and O. J. F. Martin, "Engineering the optical response of plasmonic nanoantennas," Opt. Express **16**(12), 9144–9154 (2008).
18. D. P. Fromm, A. Sundaramurthy, P. J. Schuck, G. Kino, and W. E. Moerner, "Gap-dependent optical coupling of single bowtie nanoantennas resonant in the visible," Nano Lett. **4**(5), 957–961 (2004).

#148604 - $15.00 USD Received 2 Jun 2011; revised 6 Jul 2011; accepted 14 Jul 2011; published 28 Jul 2011

19. A. Vial, A.-S. Grimault, D. Macias, D. Barchiesi, and M. L. de la Chapelle, "Improved analytical fit of gold dispersion: application to the modeling of extinction spectra with a finite-difference time-domain method," Phys. Rev. B **71**(8), 085416 (2005).

1. Introduction

Plasmonic antennas have been applied to numerous sensing, microscopy, spectroscopy and nonlinear optics experiments [1–7]. When illuminated with electromagnetic radiation of preferential wavelengths, the noble metal nanostructures which compose the antenna polarize strongly and incident electric fields can be enhanced by two orders of magnitude in the antenna gap [3]. The strong electric field enhancement allows efficient access to weak effects that would otherwise require intricate and expensive equipment to probe and detect. In combination with this, the nanoscale antenna dimensions make these devices suitable for integration into a sophisticated standalone device which may be applied to spectroscopy [2–4], clinical diagnosis [2–4], or lithography [5]. However, when the effect of interest is a molecular vibration mode in the near- or mid-infrared, antenna dimensions may increase to micrometers [2–4]. When dealing with an array of these antennas, the overall footprint can be very large, making it difficult to integrate onto a nanoscale chip. Thus, it would be desirable to red-shift the resonance of an antenna in a continuous and controllable manner over a wide range of wavelengths, while maintaining a constant antenna footprint.

One technique that has been adapted from previous developments in microwave antennas is modification of the dielectric environment of the antenna. Loading the antenna gap with another material can be used to change the broadband impedance of the antenna and shift its resonant wavelength, λ_{res} [8,9]. It has also been demonstrated that the spectral characteristics of a metal nanoshell may be tuned by varying the dielectric core material [10]. In a similar manner, a nanoshell bowtie antenna with a dielectric hole was proposed to tune the spectral response of the antenna [11]. Furthermore, it has been shown that the spectral response of a nanoshell antenna may be tuned by careful design of the geometry [12,13]. Although elegantly analogous to microwave techniques, these approaches introduce extreme fabrication constraints. Besides introducing new dielectric materials into a fabrication process, these techniques require overlay alignment (i.e. alignment between different layers of the fabrication process) that is extremely difficult with contemporary techniques. Shifting the resonance to the mid-infrared while maintaining constant antenna dimensions would require materials with extremely high ε values. It has been shown that λ_{res} of a nanoshell bowtie antenna may be tuned from λ_{res} = 635nm for a core material with ε = 1.0 to λ_{res} = 724nm for a core material with ε = 3.06. However, further increases to ε of the core material provide only marginal red-shifts to λ_{res} and a core material with ε = 5.0 shifts the wavelength only slightly to λ_{res} = 732nm [11]. Furthermore, the unavailability of materials with a continuous range of ε prevents fine-tuning of the antenna resonance while keeping the antenna size constant.

Rather than modifying the dielectric environment by introducing new materials, it is more attractive to change the geometry of the gold present in order to tune the antenna resonance conditions. In a recent investigation, it was proposed that an array of bowtie contour antennas with a contour thickness of 20nm could be used to enhance the sensitivity and reproducibility of surface-enhanced Raman scattering spectroscopy [14]. These promising results warrant a more detailed understanding of the performance of this class of antennas. In this investigation, we consider a single contour bowtie antenna, and examine the influence of the contour thickness on the antenna resonance conditions. Through these simulations, we show that it is possible to tune an antenna with a constant length over a broad spectral range, reduce the antenna footprint by a factor of 3.6, and increase the enhancement factor by 28%.

#148604 - $15.00 USD Received 2 Jun 2011; revised 6 Jul 2011; accepted 14 Jul 2011; published 28 Jul 2011

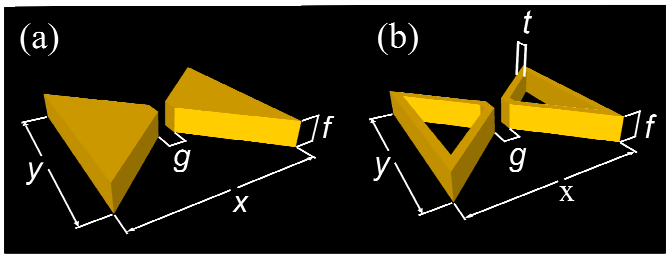

Fig. 1. Schematic representations of the simulation geometries: (a) bowtie antenna and (b) contour bowtie antenna.

2. The Contour Bowtie Antenna

A typical bowtie antenna is composed of two triangles placed in close proximity to one another. The geometry of a bowtie antenna can be characterized by four parameters, as shown in Fig. 1(a): the gap width, g; the antenna x-dimension, x; the antenna y-dimension, y; and the film thickness, f. For a conventional bowtie antenna, these parameters have been investigated in detail in previous works [15–18]. In this study, we consider two metallic triangular contours, as shown in Fig. 1(b) and use the contour thickness, t, as a tuning parameter while the antenna dimensions remain constant. Notably, the regular bowtie antenna is a special case of the contour bowtie antenna that occurs when the contour completely fills the center region. It should also be noted that the gap geometry has a significant impact on the antenna behavior. A square 30nm × 30nm (i.e. g = 30nm) gap is chosen for this investigation, as shown in Fig. 1. In addition, the gold film thickness is kept constant at f = 35nm. An antenna flare angle of 90° is used, such that $x = y$, and the antenna dimension will be referred to as x hereafter.

3. Simulation Results

A home-made, multiprocessor, three-dimensional finite-difference time-domain code is used to simulate the behavior of the contour bowtie antenna. In each simulation, a single antenna is placed on a fused silica (n_s = 1.5) substrate. The antenna material is given the broadband spectral characteristics of gold via the Drude model which has been fit to experimental data [19]. The antenna is excited from beneath the substrate with a plane wave broadband pulse and the time-domain fields in the antenna gap are recorded. The pulse was polarized along the x dimension, as shown in Fig. 1, to ensure charge accumulation adjacent to the antenna gap and strong enhancement within the gap. The broadband enhancement factor of the antenna is determined by calculating the Fourier Transform of the time-domain signal and normalizing it to the spectrum of the input pulse. A grid size of $\Delta x = \Delta y = \Delta z$ = 3nm is used and a time-step of Δt = 4.75as ensures numerical stability. A perfectly-matched layer with a geometrically-graded conductivity is used to minimize non-physical reflections at the simulation space boundaries.

3.1 Contour Thickness and Antenna Length

We investigate the behavior of this antenna first by varying the contour thickness, t, and the antenna length, x. The broadband enhancement factor for antennas with a constant length, x = 475nm, and contour thicknesses, t = {40, 60, 80}nm along with a bowtie antenna with x = 475nm is shown in Fig. 2(a). From these plots, it is evident that regardless of the thickness, t, λ_{res} of the contour bowtie antenna is always at a longer wavelength than a bowtie antenna of the same length. Furthermore, as t decreases, λ_{res} shifts to longer wavelengths and the enhancement factor increases. As the contour thickness decreases from t = 100nm to t = 30nm, λ_{res} shifts from 1.69μm to 2.42μm and the enhancement factor increases from 33.5 to 42.9. Notably, a bowtie antenna with the same dimensions has a resonance at λ_{res} = 1.40μm and an enhancement factor of 37.1. Further simulations demonstrate that a standard bowtie antenna with a length, x = 902nm, would be necessary to resonate at λ_{res} = 2.42μm. This

#148604 - $15.00 USD Received 2 Jun 2011; revised 6 Jul 2011; accepted 14 Jul 2011; published 28 Jul 2011

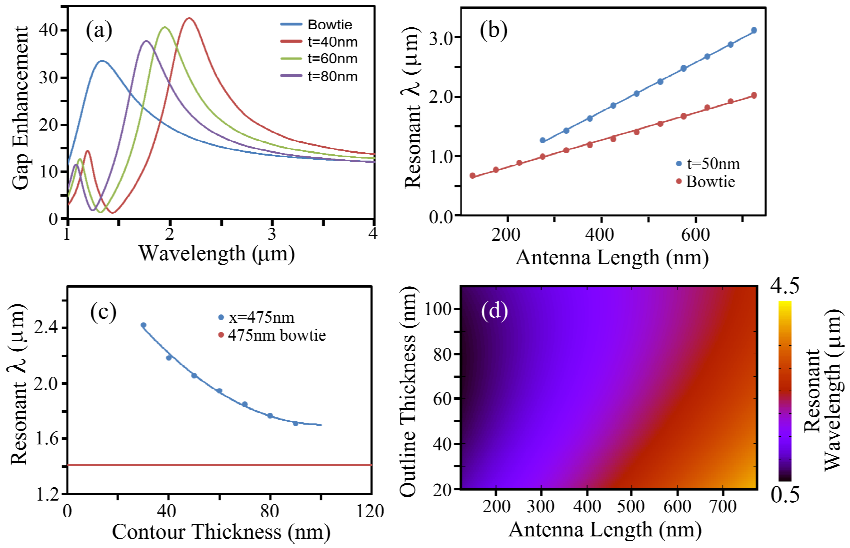

Fig. 2. (a) Broadband enhancement factors for a bowtie antenna and contour bowtie antennas with t = {40,60,80}nm and a length, x = 475nm. (b) λ_{res} versus antenna length for a bowtie antenna and a t = 50nm contour bowtie antenna, each with a length, x = 475nm. (c) λ_{res} versus contour thickness, t, for an antenna length, x = 475nm. λ_{res} for a bowtie antenna with x = 475nm is shown for reference. (d) Paraboloid fit to 70 simulated data points relating λ_{res} to $\{x,t\}$.

demonstrates that the contour bowtie antenna can be used to decrease x by a factor of 1.90, decrease the footprint by a factor of 3.60, and increase the enhancement by 28%.

Interestingly, these results demonstrate that the contour bowtie antenna behaves in the same way as a plasmonic nanoshell. In the case of a nanoshell, it has been shown that the plasmon resonance depends on the radius of the core material and on the thickness of the gold nanoshell. Increasing the radius of the core material (analogous to increasing the antenna dimensions) red-shifts the resonance, whereas increasing the nanoshell thickness (analogous to increasing t) blue-shifts the resonance [10]. Furthermore, it has been demonstrated in previous works that decreasing the antenna gap dimension yields greater electric field enhancement [18]. Decreasing the thickness, t, increases λ_{res} of the antenna and the gap dimension relative to λ_{res} decreases. As a result, decreasing t produces greater enhancement in the antenna gap. Such a significant increase in λ_{res} and enhancement factor would be unattainable by loading a nanoshell bowtie antenna with a dielectric, as discussed in the introduction [11].

The broadband tunability of these antennas is demonstrated by simulating a wide range of antenna lengths, x, and contour thicknesses, t. The wavelength of the primary resonance is

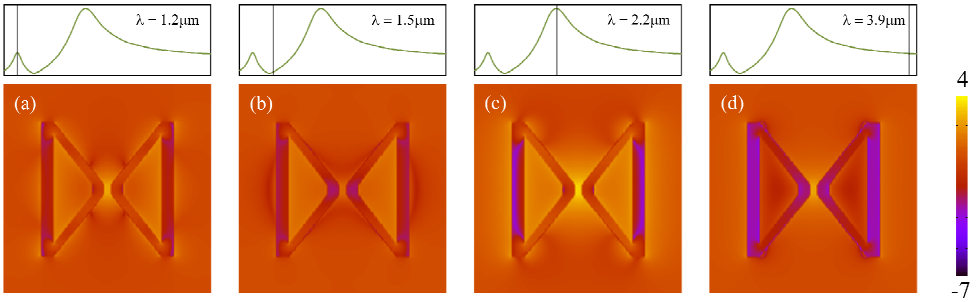

Fig. 3. Logarithmic scale intensity distributions at spectral points of interest: (a) Secondary resonance at λ = 1.2μm, (b) anti-resonance at λ = 1.5μm, (c) primary resonance at λ = 2.2μm, and (d) above resonance at λ = 3.9μm.

#148604 - $15.00 USD Received 2 Jun 2011; revised 6 Jul 2011; accepted 14 Jul 2011; published 28 Jul 2011

calculated for 70 antennas with lengths spanning 175nm ≤ x ≤ 725nm in 50nm steps and contour thicknesses spanning 30nm ≤ t ≤ 100nm in 10nm steps. Figure 2(b) shows a typical plot of λ_{res} versus x for t = 50nm. The length trend for a bowtie antenna is shown for comparison. Evidently, the relationship is linear and the operating wavelength of the contour bowtie antenna is higher than the bowtie antenna for each of the antenna lengths simulated. Interestingly, as the antenna length decreases, the empty space in the center region of the antenna begins to fill and it starts to resemble a bowtie antenna. These two lines intersect at x = 141nm, which is the point where the center of the contour bowtie antenna is completely filled and its behavior converges to that of the bowtie antenna. Similarly, the dependence between contour thickness, t, and λ_{res} is plotted in Fig. 2(c). This trend is parabolic, which shows that λ_{res} is directly proportional to the area removed from the center of the antenna. Building on Figs. 2(b) and 2(c), a paraboloid of the form $\lambda = c_1x^2 + c_2x + c_3t^2 + c_4t + c_5xt + c_6$ is fit to 70 data points for various values of x and t with $\{c_1,c_2,c_3,c_4,c_5,c_6\} = \{6.75 \times 10^{-4}, 4.55, 0.129, -17.2, -2.01 \times 10^{-2}, 765\}$ and $R^2 = 0.999$. A surface plot of this fit is shown in Fig. 2(d).

In order to understand the behavior of the antenna, it is useful to plot the intensity distribution at points of interest in its spectrum. The intensity distribution for a contour antenna with x = 475nm and t = 40nm is plotted at its secondary resonance (λ = 1.2μm) in Fig. 3(a), its anti-resonance (λ = 1.5μm) in Fig. 3(b), its primary resonance (λ = 2.2μm) in Fig. 3(c), and above λ_{res} (λ = 3.9μm) in Fig. 3(d). When excited on-resonance, the intensity distributions show that the antenna is strongly polarized and incident energy is confined to the gap. By controlling the incident electric field intensity, all sensitive processes can be made to originate from the antenna gap, making this design suitable for probing a small number of atoms or molecules localized to the gap region. When excited at its anti-resonance, fields are slightly enhanced in the hollow region of the antenna, while fields in the gap experience only minimal enhancement. Although enhancement is observed in the gap when the antenna is excited above λ_{res}, there is minimal interaction with the remainder of the antenna. Examination of Fig. 3(c) reveals that the interaction of the radiation with the vertical edge on-resonance is notably different than with the other edges. Additionally, there is moderate electric field enhancement in the hollow region of the antenna. Therefore, it would be interesting to isolate the vertical edge and examine its influence on the resonance conditions of the antenna. This is done by two separate studies: (1) Varying only the thickness of the vertical edge while maintaining the thickness of the other edges constant; and (2) Displacing the vertical edge towards the center of the antenna.

3.2 Vertical Edge Thickness

In order to investigate the influence of the vertical edge thickness, t_v, the thickness of the two diagonal edges is maintained constant at t = 30nm, the antenna length is kept constant at x = 475nm, and the thickness of the vertical edge is varied between 0nm ≤ t_v ≤ 150nm. A schematic depiction of this geometry is shown in Fig. 4(a). The effect of the edge thickness on λ_{res} is presented in Fig. 4(b). In a similar manner as increasing the contour thickness (shown in Fig. 2(c)) in a uniform manner decreases λ_{res}, so does increasing only the vertical edge thickness. However, in this case λ_{res} decreases linearly with the vertical edge thickness. For a uniform edge thickness, each infinitesimal increase in t produces a greater change to the geometry than increasing t_v. The convergence of the geometry to that of the bowtie antenna is approximately linear when only t_v is increased, yielding the linear trend in Fig. 4(b).

3.3 Vertical Edge Displacement

A typical example of this geometry is shown in Fig. 4(c). The antenna length is kept constant at x = 475nm, while the vertical edge is shifted towards the center of the antenna by a distance, d. The relationship between d and λ_{res} is shown in Fig. 4(d). Interestingly, as d increases, the useful area of the antenna effectively shrinks and λ_{res} decreases up to d = 80nm.

#148604 - $15.00 USD Received 2 Jun 2011; revised 6 Jul 2011; accepted 14 Jul 2011; published 28 Jul 2011

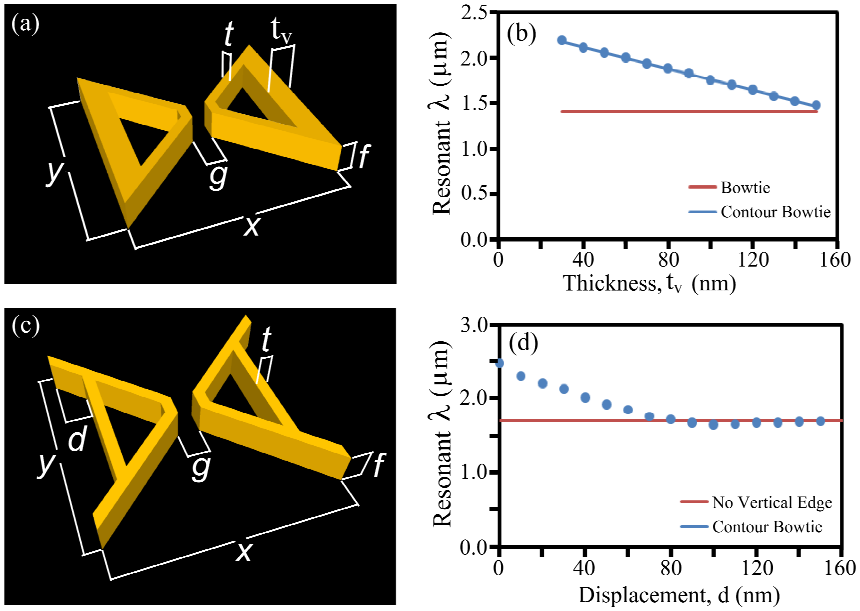

Fig. 4. (a) Schematic representation of a contour bowtie antenna with $t_v \neq t$. (b) λ_{res} versus t_v for $\{x,t\} = \{475,30\}$nm. λ_{res} for a bowtie antenna is shown for reference. (c) Schematic representation of a contour bowtie antenna with a shifted vertical edge. (d) λ_{res} versus edge displacement, d. The case when the vertical edge is removed altogether is shown for reference.

To illustrate this, we consider d = 50nm. The vertical edges of both the left and right contours are shifted inwards, so their combined shift is $2d$ = 100nm. Interestingly, λ_{res} of a normal contour bowtie antenna with t = 30nm and x = 375nm is almost identical at λ_{res} = 1940nm, indicating that the corner segments extending beyond the vertical edge do not interact with incident radiation at resonance. The situation changes as the vertical edge is shifted beyond 80nm and λ_{res} saturates and approaches λ_{res} = 1692nm when d = 150nm. When the vertical edge is removed altogether, λ_{res} = 1696nm and the gap enhancement decreases only slightly to 41.2, demonstrating that the antenna is still somewhat functional without the vertical edge and that as the vertical edge is shifted beyond d = 80nm, it interacts only minimally with the incident radiation. Based on these observations, the placement of the vertical edge as shown in Fig. 1(b) is the optimal case for this antenna design.

4. Conclusion

In summary, we have numerically simulated the operation of a class of plasmonic antennas over a wide space of parameters. These results demonstrate that these antennas offer more compact dimensions when compared to a bowtie antenna and that the operating wavelength of the antenna may be tuned over a wide range by changing the contour thickness, t, while maintaining a constant antenna footprint. Increasing the antenna length and decreasing the contour thickness both act to red-shift the antenna resonance conditions. Both the thickness of the vertical edge of the antenna and its position are found to be very important for optimizing the antenna performance. It is anticipated that these results will inspire further developments in plasmonic antennas with complex geometries and will have future applications in near- to mid-infrared spectroscopy and sensing.

Acknowledgments

This work was supported by the Natural Sciences and Engineering Research Council of Canada, Alberta Innovates, and the Canadian Research Chairs Program.

#148604 - $15.00 USD Received 2 Jun 2011; revised 6 Jul 2011; accepted 14 Jul 2011; published 28 Jul 2011